

Probing the domain structure of FtsZ by random truncation and insertion of GFP

Masaki Osawa and Harold P. Erickson

Dept of Cell Biology, 3709 Duke University Medical Center, Durham, NC 27710, USA

Correspondence
Harold P. Erickson
H.Erickson@cellbio.duke.edu

Received 24 May 2005
Revised 24 August 2005
Accepted 12 September 2005

Random transposon-mediated mutagenesis has been used to create truncations and insertions of green fluorescent protein (GFP), and Venus-yellow fluorescent protein (YFP), in *Escherichia coli* FtsZ. Sixteen unique insertions were obtained, and one of them, in the poorly conserved C-terminal spacer, was functional for cell division with the Venus-YFP insert. The insertion of enhanced GFP (eGFP) at this same site was not functional; Venus-YFP was found to be superior to eGFP in other respects too. Testing the constructs for dominant negative effects led to the following general conclusion. The N-terminal domain, aa 1–195, is an independently folding domain that can poison Z-ring function when expressed without a functional C-terminal domain. The effects were weak, requiring expression of the mutant at 3–5 times the level of wild-type FtsZ. The C-terminal domain, aa 195–383, was also independently folding, but had no activity *in vivo*. The differential activity of the N- and C-terminal domains suggests that FtsZ protofilament assembly is directional, with subunits adding primarily at the bottom of the protofilament. Directional assembly could occur by either a treadmilling or a dynamic instability mechanism.

INTRODUCTION

FtsZ is the major cytoskeletal protein in bacterial cell division. FtsZ forms a ring at the centre of the cell, visible by fluorescence microscopy (Levin & Losick, 1996; Ma *et al.*, 1996), that constricts as the cell divides. The substructure of the ring is inferred from *in vitro* studies. In appropriate buffers and in the presence of GTP, FtsZ assembles into protofilaments that are one subunit thick (Chen *et al.*, 2005; Erickson *et al.*, 1996; Romberg *et al.*, 2001). Under some conditions the protofilaments associate to form pairs, sheets or bundles, but the basic assembly unit appears to be the single protofilament (Chen *et al.*, 2005). We believe that the Z ring seen by light microscopy is assembled from overlapping short protofilaments, and is only 2–3 or 6–9 protofilaments thick, depending on the species and strain (Anderson *et al.*, 2004; Chen & Erickson, 2005).

Oliva *et al.* (2004) have recently provided evidence that FtsZ comprises two globular domains that fold independently. The N-terminal globular domain includes the GTP-binding site and all the residues in the top protofilament interface. The C-terminal globular domain includes all the residues on the bottom protofilament interface. Following this C-terminal domain is a segment that is poorly conserved, and of variable length, across different bacterial species, and this is followed by a short peptide that is highly conserved. This highly conserved C-terminal peptide is the binding site for

FtsA and ZipA (reviewed by Vaughan *et al.*, 2004). In *Mycobacterium*, which has no FtsA or ZipA, this peptide binds FtsW (Datta *et al.*, 2002), and may do so in other species. The variable segment has been thought to serve as a flexible tether or spacer between the C-terminal globular domain and the C-terminal peptide (Erickson, 2001; Vaughan *et al.*, 2004).

A recent study explored point mutants of the top and bottom protofilament interfaces (Redick *et al.*, 2005). Mutations on the bottom interface were dominant negative when expressed at 3–5 times the level of wild-type FtsZ. Mutations on the top interface were not dominant negative, even at 5 times wild-type levels. As discussed later, this suggested a directional assembly mechanism, where subunits add primarily to the bottom of a protofilament.

We decided to explore the surfaces of FtsZ and its domain structure using a transposon reaction to insert an entire green fluorescent protein (GFP) molecule at random locations. This technique was developed by Sheridan *et al.* (2002), and produced 12 in-frame insertions in the G protein subunit α_s . Two of them retained α_s function. When applied to the glutamate receptor GluR1, a ~100 kDa transmembrane protein, 35 unique in-frame insertions were obtained, and 6 were at least partially functional (Sheridan *et al.*, 2002).

We had two goals in applying the insertion technique to FtsZ. First, we hoped to find a site where a GFP could be inserted and not block FtsZ function. Previous GFP fusions

Abbreviations: eGFP, enhanced green fluorescent protein; GFP, green fluorescent protein; YFP, yellow fluorescent protein.

at the N- or C-terminus of FtsZ could only be used as labels when the fusion protein was expressed as a fraction of the native FtsZ; they could not function as the sole source of FtsZ. The second goal was to test all the truncations and insertions for their ability to poison cell division by interfering with wild-type FtsZ. This should provide a map of domain activity.

METHODS

In vitro transposon reaction. The transposon vectors were kindly provided by Dr Thomas E. Hughes, Yale University, New Haven, CT, USA. The original vector pBNJ24.6 contained enhanced GFP (eGFP). We made a new vector in which the eGFP was replaced with the yellow fluorescent protein (YFP) variant Venus, which was kindly provided by Dr Atsushi Miyawaki, RIKEN, Japan (Nagai *et al.*, 2002). A PCR product of YFP (forward primer, AAAGGCGCGCCGTG-AGCAAGGGCGAGGAGCT; reverse primer, AAGGCGCGCCCT-TGTACAGCTCGTCCATGC) was inserted between the *Ascl* sites. The transposon insertion reaction was carried out as described by Sheridan *et al.* (2002), and also following a detailed protocol provided by Dr Thomas E. Hughes. The transposon was amplified by PCR using a single primer derived from the mosaic-end sequence (CTGTCTCTTATACACATCT), and the product (200 ng) and 60 ng

pJSB100 (pJSB2 expressing wild-type FtsZ; Redick *et al.*, 2005) were mixed with transposase (Epicentre). After inactivation of the transposase by 1% SDS and heating to 80 °C for 10 min, a high efficiency electro-competent strain, STBL4 (Invitrogen), was transformed with the products. Kanamycin-resistant clones were selected on LB agar plates containing 50 µg kanamycin ml⁻¹. In addition to the transposon-derived truncation chimeras, we generated four C-terminal truncations (aa 1–158, 1–173, 1–195 and 1–239) and one N-terminal truncation (aa 195–383) with no YFP/GFP. Three GFP insertions at aa 1, 333 and 348 were also replaced with Venus-YFP, using the *Ascl* sites (Fig. 1), to compare GFP and YFP insertions.

Complementation and dominant negative assays. The complementation and dominant negative assays were performed as described by Stricker & Erickson (2003), and Redick *et al.* (2005). *Escherichia coli* strains JKD7-1 (Dai & Lutkenhaus, 1991) and BW27783 (Khlebnikov *et al.*, 2001) were used as hosts for the complementation and dominant negative assays, respectively.

Microscopy. BW27783 cells expressing truncated FtsZ with YFP/GFP following the truncation were grown in 0.002% or 0.0002% arabinose until the OD₆₀₀ value reached 0.5–0.7, then were fixed with 2.6% paraformaldehyde for 15 min at room temperature and incubated on ice for 1 h. Cells were visualized with differential-interference contrast and fluorescence microscopy using a Zeiss Axiophot with a 100 × N.A. 1.3 objective lens. Filter cubes optimized for YFP and GFP were used for fluorescence microscopy. Images were

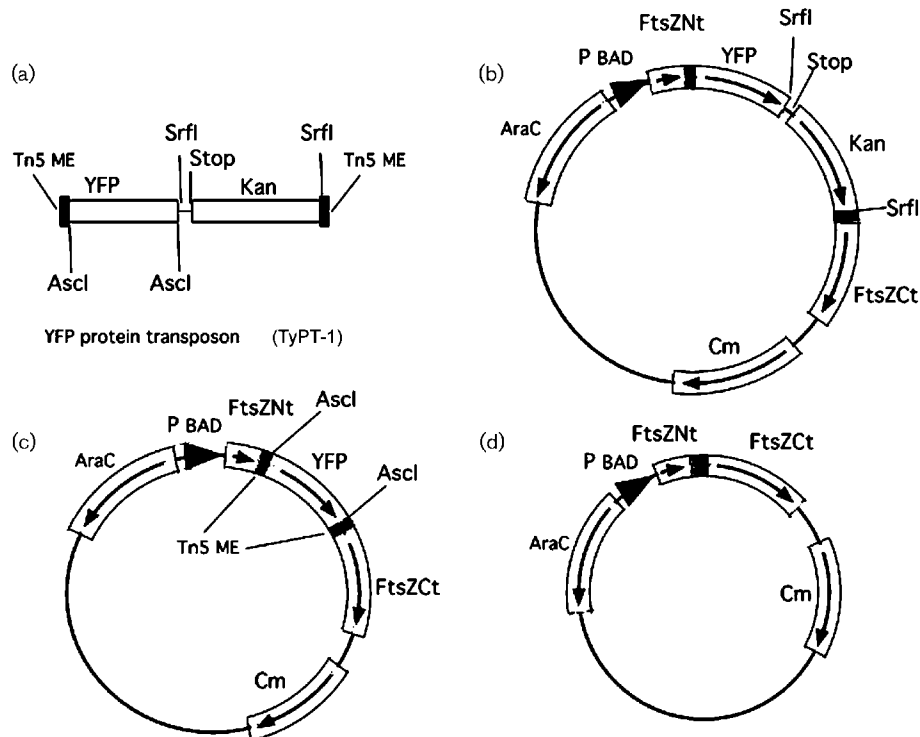


Fig. 1. Diagrams of the Tn5 transposon and the three constructs obtained from it. (a) The Tn5 transposon construct contains mosaic ends (MEs) at each end flanking the YFP, an in-frame stop and a Kan^r cassette. (b) The insertion reaction produces a modified pJSB2-FtsZ in which the entire transposon construct is inserted randomly into the FtsZ coding segment. Because the construct has an in-frame stop following the YFP, this vector will produce a truncated FtsZ with YFP at the C-terminus. (c) The stop-Kan^r segment is flanked by *Srfl* sites, which permit its removal, leaving a full-length FtsZ with the YFP inserted. The YFP is flanked by 7 aa tails corresponding to the ME segments, and these are flanked by a 3 aa repeat of the FtsZ sequence at the insert site. (d) The YFP insert can be removed by cutting with *Ascl* and religating. This leaves a 20 aa insert corresponding to the ME, restriction site and the 3 aa repeat.

acquired with a Coolsnap HQ CCD camera (Roper Scientific). BW27783 cell lengths were measured for each mutant, and the results reported as the mean \pm SD.

RESULTS

Making the deletion and insertion constructs

We did two separate transposon reactions, one with the YFP variant Venus (Nagai *et al.*, 2002), which we will hereafter refer to as YFP, and one with eGFP, which we will hereafter refer to as GFP. The transposon insertion reaction produced pBAD-based expression vectors with random insertions of YFP/GFP-Kan^r (Fig. 1a) within the FtsZ coding region, as illustrated in Figs 1(b) and 2(a). Following the insertion reaction, clones were selected by plating on kanamycin and chloramphenicol, and each clone was checked for fluorescence. Clones (260) from the GFP reaction were screened, and 6 showed fluorescence. DNA restriction analysis showed that all six had GFP inserted in the FtsZ coding region. Clones (180) from the YFP reaction were screened, and 16 showed fluorescence. Thirteen of these had YFP inserted in the FtsZ coding region (the other three were presumably inserted somewhere else in the vector that permits expression, such as in the *AraC* cDNA). Three of the insertion sites were obtained twice, so we had sixteen unique insertions to investigate.

At this first stage of mutagenesis each fluorescent clone expressed an N-terminal portion of FtsZ fused in-frame to YFP or GFP (Fig. 1b and 2a). We refer to these as C-terminal truncation chimeras, or del-YFP/GFP. We then derived two additional constructs from each clone. First, we removed the Kan^r cassette, along with the stop codon following the YFP/GFP. This reunited the C-terminal segment of FtsZ leaving the YFP/GFP as an insert in the full-length FtsZ (Figs 1c and 2b). Second, we removed the YFP/GFP, leaving a much smaller 20 aa insert (Figs 1d and 2c). We now had 16 sites in FtsZ with (a) a C-terminal truncation fused to YFP/GFP, (b) a large YFP/GFP insert or (c) a small 20 aa insert. Insertion

sites were identified by the 3 aa sequence that is repeated before and after the insert, e.g. 193VQG195 (Table 1).

In addition to the transposon-generated constructs, we prepared a construct with a YFP insert at aa 326, and another construct with YFP fused to the C-terminus (FtsZ-YFP), and included these in the analysis. Also, we prepared several C-terminal deletions and one N-terminal deletion that had no GFP. Most important are the ones that we call the N-terminal domain, aa 1–195, and the C-terminal domain, aa 195–383.

Testing the constructs for complementation

The C-terminal truncation chimeras (we checked only deletions 377, 348 and 333) were not able to complement the *ftsZ* null mutant strain. This was not surprising since they are all missing the essential C-terminal peptide that binds ZipA and FtsA. We then removed the Kan^r and stop codon, leaving the YFP/GFP as an insert in the full-length protein. None of these YFP/GFP inserts in FtsZ complemented (we tested all 16, plus the YFP insert at aa 326 and the C-terminal YFP constructs). We also tested the constructs with the smaller 20 aa inserts and found one that could complement, which has an insert at 331VQQ333 in the C-terminal spacer.

Since FtsZ with a 20 aa insert at this site was functional, but FtsZ with a GFP insert was not, we became suspicious that the GFP might itself be the cause of the disruption. We therefore replaced the GFP with YFP (Venus), because this YFP is reported to have better folding properties than GFP (Nagai *et al.*, 2002). This construct with the YFP insertion at 331VQQ333 (333ins-YFP) complemented, although with some complications. The right number of colonies appeared on the complementation plate, but growth was slower than for wild-type FtsZ. After 16 h small colonies appeared of uniform size and shape. At random times over the next 24 h colonies started growing faster, developing a larger and irregular shape. Eventually, the colonies showed a wide range of sizes and shapes. This might have been due to a second mutation occurring at relatively high frequency

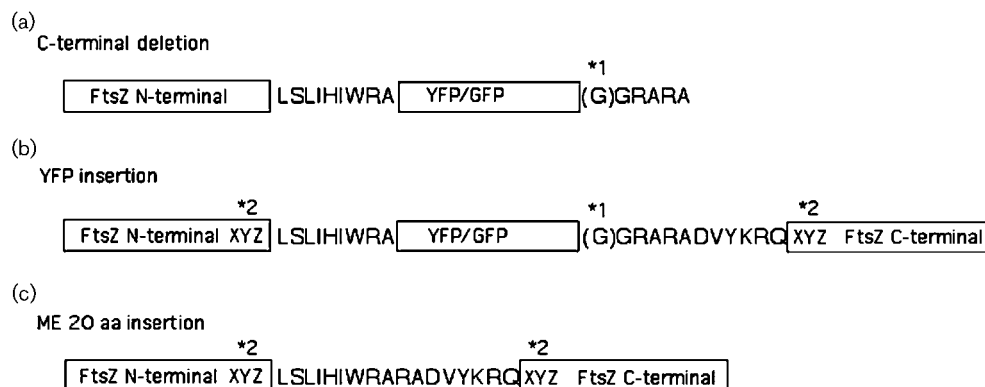


Fig. 2. Details of the sequence at the insertion and deletion sites. *1, This G was eliminated for the YFP construct. *2, Three amino acids in FtsZ were repeated at the beginning and end of the insertion.

Table 1. Summary of physiological activity of the mutants

Construct name	Insertion site*	GFP localization (0.002% arabinose)†	Dominant negative			
			Cell elongation (μm) at 0.0002 (0.002)% arabinose	Colony formation‡		Streak (0.0002% arabinose)§
				0.002% Arabinose	0.02% Arabinose	
Mock (pJSB2)			2.0 \pm 0.3 (1.8 \pm 0.7)	–	–	–
Wild-type FtsZ			2.5 \pm 0.6 (3.2 \pm 1.6)	–	–	–
FtsZ-YFP (Nt fusion)		Z	2.1 \pm 0.7 (3.0 \pm 0.9)	–	–	–
FtsZ-YFP (Ct fusion)		Z	3.1 \pm 1.0 (8.9 \pm 3.6)	–	–	–
N-term domain (1–195)			18.0 \pm 5.4	sm col	no col	+
C-term domain (195–383)			2.2 \pm 0.8 (2.6 \pm 0.8)	–	–	–
del-GFP	–2HPM1	Diffuse	1.9 \pm 0.6	–	–	–
ins-GFP		Z	6.1 \pm 3.1	–	–	–
ins-YFP		Z	2.1 \pm 0.7	–	–	–
ins-20aa				–	–	–
del-GFP	6ELT8	Diffuse/foci	2.0 \pm 0.4	–	–	–
ins-GFP	Bottom	Diffuse/foci	24.4 \pm 6.6	sm col	sm col	+
ins-20aa				sm col	sm col	+
del-YFP	96DMV98	Diffuse/foci	2.1 \pm 0.7	–	–	–
ins-YFP	Bottom	Diffuse/foci	2.8 \pm 0.7	–	–	–
ins-20aa				–	–	–
del-YFP	132TKP134	Diffuse/foci	2.0 \pm 0.6	–	–	–
ins-YFP	Top	Diffuse/foci	2.8 \pm 0.5	–	–	–
ins-20aa				–	–	–
del-YFP	139GKK141	Diffuse/foci	2.9 \pm 1.5	–	–	–
ins-YFP	Top	Diffuse/foci	3.0 \pm 0.8	–	–	–
ins-20aa				–	–	–
del-YFP	156HVD158	Diffuse/foci	2.7 \pm 1.1	–	–	–
ins-YFP	Front (middle)	Diffuse/foci	2.6 \pm 0.7	–	–	–
ins-20aa				–	–	–
C-term del	1–158		2.2 \pm 0.6	–	–	–
del-YFP	171VLG173	Diffuse/foci	2.8 \pm 0.7	–	–	–
ins-YFP	Right (top)	Diffuse/foci	2.8 \pm 0.6	–	–	–
ins-20aa				–	–	–
C-term del	1–173			–	–	–
del-YFP	193VQG195	Diffuse/foci	3.1 \pm 1.3	–	–	–
ins-YFP	Buried (H7)	Diffuse/foci	10.5 \pm 3.2	sm col	sm col	+
ins-20aa				sm col	sm col	+
C-term del	1–195		18.0 \pm 5.4	sm col	no col	+
del-YFP	212DVR214	Weak Z/foci	12.0 \pm 3.2	sm col	sm col	+
ins-YFP	Bottom	Diffuse/foci	22.6 \pm 4.3	no col	no col	+
ins-20aa				no col	no col	+
del-GFP	232GED234	Weak Z/foci	21.7 \pm 6.1	sm col	sm col	+
ins-GFP	Right	Diffuse/foci	18.9 \pm 5.5	sm col	sm col	+
ins-20aa				sm col	sm col	+

Table 1. cont.

Construct name	Insertion site*	GFP localization (0.002 % arabinose)†	Dominant negative			
			Cell elongation (μm) at 0.0002 (0.002) % arabinose	Colony formation‡		Streak (0.0002% arabinose)§
				0.002 % Arabinose	0.02 % Arabinose	
del-YFP	237EEA239	Weak Z/foci	18.2 ± 3.8	no col	no col	+
ins-YFP	Right	Diffuse/foci	19.1 ± 6.0	sm col	sm col	+
ins-20aa				sm col	sm col	+
C-term del	1–239		55.8 ± 10.6	no col	no col	+
del-YFP	246SPL248	Weak Z/foci	12.8 ± 4.0	sm col	no col	+
ins-YFP	Right	Diffuse/foci	19.3 ± 5.1	sm col	sm col	+
ins-20aa				–	–	–
del-YFP	286ASD288	Diffuse/foci	16.2 ± 5.0	sm col	sm col	+
ins-YFP	Bottom/front	Diffuse/foci	17.9 ± 2.9			
ins-YFP	326V	Z	17.2 ± 3.6	sm col	sm col	
del-GFP	331VQQ333	Weak Z/foci	15.2 ± 5.2	sm col	sm col	+
ins-GFP		Weak Z/foci	21.5 ± 4.0	sm col	sm col	+
ins-YFP		Z	10.3 ± 3.7	–	sm col	
ins-20aa				–	–	–
del-GFP	346PLT348	Weak Z/foci	16.4 ± 5.3	sm col	sm col	+
ins-GFP		Weak Z/foci	21.7 ± 7.1	sm col	sm col	+
ins-YFP		Z	22.0 ± 6.8	sm col	sm col	
ins-20aa				sm col	sm col	+
del-YFP	375PAF377	Z	15.4 ± 3.8	sm col	sm col	+
ins-YFP		Z	24.0 ± 5.9	sm col	sm col	+
ins-20aa				sm col	sm col	+

*The 3 aa repeat at the insertion site is indicated. Top indicates the upper protofilament interface, equivalent to the plus end of a microtubule. Front, right, etc. indicates the view of the protofilament from outside a microtubule, plus end up.

†Z, indicates localization at the Z ring; foci, indicates small bright spots.

‡sm col, indicates that small colonies were obtained; no col, indicates that no colonies were formed; –, no effect (normal growth).

§+, dominant negative effect (no growth); –, no effect (normal growth).

elsewhere in the genome, at random times after a small colony had formed. Cells were picked from both the small uniformly sized colonies and the large irregularly shape colonies, and were induced with 0.2–0.02 % arabinose in liquid culture at 42 °C. Cells derived from both colonies were identical in appearance, showing many normal short cells with a single Z ring (Fig. 3). The cells derived from large irregular colonies probably harbour a second mutation. The cells from small colonies may have acquired the second mutation in the liquid culture.

We also tested the replacement of GFP with YFP at aa 348. The YFP insert construct did not complement, which was not unexpected since the 20 aa insert also did not complement at this position. However, the YFP insert protein

showed a much stronger and sharper localization to the Z ring than the GFP construct protein (discussed below).

Testing the constructs for dominant negative effects

To test the constructs for dominant negative effects, it was important first to establish that the proteins were being expressed. We used 0.002 % arabinose in liquid culture for 80 min at 37 °C to induce the expression of the proteins from pJSB2 in *E. coli* BW27783, which we had previously found to give near maximal expression and a level about 3–5 times that of the genomic FtsZ (Redick *et al.*, 2005). Cultures were centrifuged and the cell pellets were lysed with SDS sample buffer, and the total protein concentration was



Fig. 3. Z rings in a strain with the YFP insertion at FtsZ aa 333 as the sole source of FtsZ. The cells were derived from a colony after it had transformed into the fast growing and irregularly shaped type, and cultured at 42 °C in LB containing 0.2% arabinose.

determined by the Bradford assay (Bio-Rad). The samples were analysed by SDS-PAGE and immunoblotting. The proteins were detected with anti-FtsZ antibodies and visualized with an ECL kit (Amersham). Fig. 4(b) shows Western blots of proteins from cells expressing the C-terminal truncation chimeras. All constructs were expressed at about 3–5 times the level of genomic FtsZ.

Fig. 4(c) shows the test of truncation chimeras for dominant negative effects, in which cells were streaked on agar plates with 0.0002% and 0.002% arabinose (arabinose concentrations below 0.0002% showed no dominant negative effects for several mutants tested); these should express the mutant protein at ~1 and 3–5 times the level of the endogenous FtsZ, respectively (Redick *et al.*, 2005). The results were identical at both concentrations. All the strains containing truncation chimeras in the N-terminal domain (Fig. 4a), up to aa 195, showed growth equivalent to wild-type cells, i.e. they had no dominant negative effects. All truncation chimeras in the C-terminus, from aa 214 onward to the C-terminus, showed dominant negative inhibition of growth. Fig. 4(d) shows the same test for full-length FtsZ with YFP/GFP insertions. With the exceptions of aa 1, 8 and 195, the insertions behaved the same as the truncation chimeras in the dominant negative assay.

We also checked for dominant negative effects using a colony formation assay. This assay is more quantitative since one can score for colony size and the absence of colonies at different arabinose concentrations. There was generally good qualitative agreement between the streaking and colony assays, in that every clone judged dominant negative in the streaking assay gave either smaller colonies or no colonies (Table 1). In the colony assay no dominant negative effects were seen at 0.0002%. We obtained small colonies and sometimes no colonies at 0.002% and 0.02% arabinose, which induces expression of the mutant protein at 3–5 times

the wild-type level. Note that growth inhibition required a 10 times higher concentration of arabinose in the colony assay than in the streaking assay; we do not know the reason for this. The streaking assay corresponds more closely to cell elongation in liquid culture, at 0.0002% arabinose (see below). Colony growth is not very sensitive to effects on cell elongation.

Effects of dominant negative mutants on cell length and localization of del-YFP/GFP chimeras

We examined cells under dominant negative conditions in liquid culture (Fig. 5). Truncation chimeras in the N-terminal domain had no effect on cell length, compared with the controls (Fig. 5 a, b), while all truncation chimeras beyond aa 195 produced elongated cells, at both 0.0002% and 0.002% arabinose. The N-terminal domain (aa 1–195) produced cell elongation even at the lower arabinose concentration (Fig. 5 d), while the C-terminal domain (aa 195–383) showed no effect at the higher arabinose concentration Fig. 5(c). Truncation chimeras in the supposedly flexible spacer also produced cell elongation (Table 1).

We tested two of the truncation mutants, 1–195 (the N-terminal globular domain) and 1–239, which had the most potent dominant negative effects in the colony assay, over a more extensive range. Both gave continuous growth in liquid culture at 0.0002% arabinose (expression induced at ~1 times the wild-type level of FtsZ; Redick *et al.*, 2005). Mutant 1–195 had a normal doubling time of 28 min, while 1–239 had a doubling time of 40 min. Both had highly elongated cells at this concentration. At 0.00005% arabinose (expression induced at ~0.3 times the wild-type level of FtsZ) 1–195 had somewhat elongated cells while 1–239 were more highly elongated, and the doubling times of both were normal.

We examined the localization of truncation-chimera proteins and YFP/GFP-insert proteins under dominant negative conditions. The insert at aa 1 (GFP-FtsZ) localized to the Z ring at 0.0002% arabinose, as previously reported for N-terminal GFP (Ma *et al.*, 1996), and produced aberrant rings and elongated cells at higher arabinose. When GFP was replaced with YFP at –2HPM1 (Nt-YFP fusion), cells expressing it were short and showed sharp Z rings even in 0.002% arabinose (Fig. 5e). FtsZ with YFP at the C-terminus (Ct-YFP fusion) gave similar sharp localization at 0.0002% (Fig. 5f). At 0.0002% or 0.002% arabinose, the Ct-YFP fusion formed variably elongated cells, some with multiple Z rings (Fig. 5f, g). The N-terminal YFP fusion was distinctly dimmer than the C-terminal fusion, and we believe that this protein is expressed at lower levels than the C-terminal fusion. Truncations and insertions from aa 98 to 173 gave a mostly diffuse localization with some bright foci (Fig. 5i). Truncation chimeras at aa 214 and beyond showed a tendency to make clusters with a periodicity similar to that of multiple Z rings at 0.002% arabinose (Fig. 5j). The clusters were much more diffuse than Z rings and may

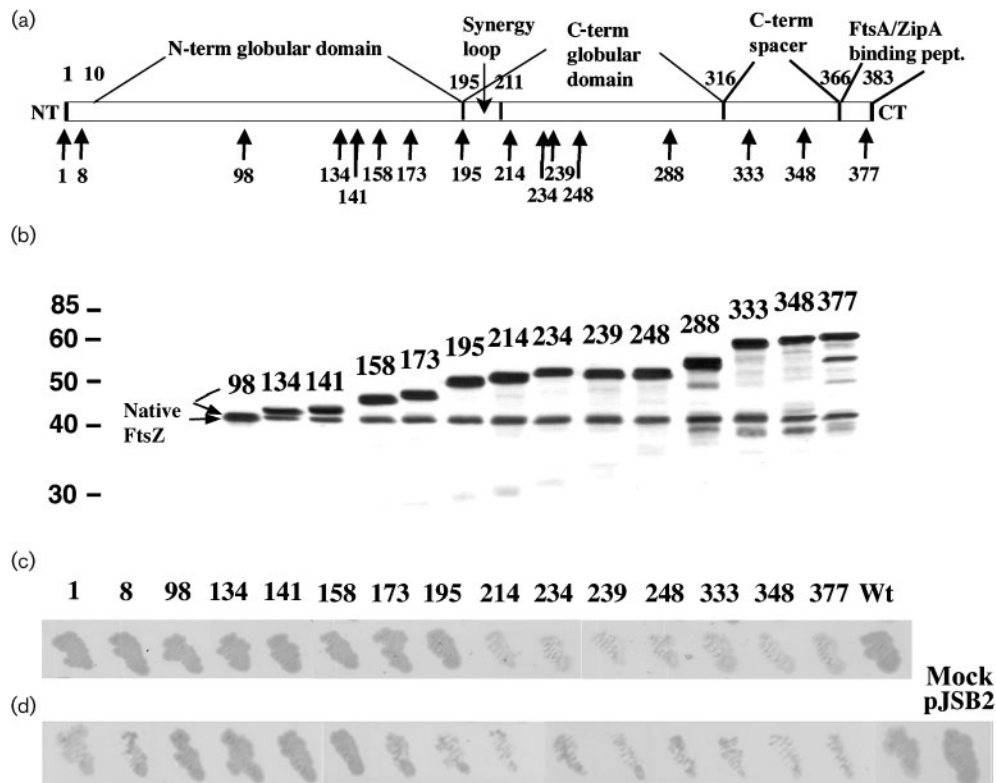


Fig. 4. Analysis of deletion chimeras. (a) Schematic illustration of transposon insertion sites. The nomenclature we use for FtsZ domains is also indicated. The N-terminal globular domain (aa 10–195) is the Rossman fold, and contains the GTP-binding site and all the amino acids of the upper protofilament interface. This domain also includes about 2/3 of helix H7, through aa 195, which makes contact with the Rossman fold. The C-terminal globular domain is from aa 195–316. This domain includes the synergy or T7 loop (Erickson, 1998; Nogales *et al.*, 1998) on the bottom interface. The C-terminal spacer, aa 317–366, is a segment of variable length with little sequence conservation – it is thought to be a flexible tether. At the very C-terminus is a short peptide (aa 367–383), highly conserved in almost all FtsZ proteins (Erickson, 2001; Vaughan *et al.*, 2004), that binds FtsA and ZipA. Arrows below the line show the sites of our inserts and the numbers indicate the last amino acids in the 3 aa repeat. (b) Western blot showing the expression of C-terminal truncation chimeras. Immunoblotted proteins were analysed with anti-FtsZ antibodies. Anti-GFP antibodies showed similar results (data not shown). The numbers above the lanes indicate the truncation sites and the sizes of the molecular mass markers (kDa) are shown on the left. (c) Testing C-terminal truncation chimeras for dominant negative effects. Cells were streaked on LB agar plates containing 0.002% arabinose. Normal growth produced a dark patch, and dominant negative constructs produced a lighter patch (inhibited growth). (d) A similar test of the YFP/GFP insertion mutants. In this figure we tested GFP insertions at aa 1, 333 and 348.

represent concentration of FtsZ by nucleoid exclusion (Harry, 2001; Margolin, 2001). The cells still elongated at 0.0002% arabinose but the clusters were not observed (Fig. 5k). All four YFP insertions in the spacer and C-terminal peptide showed sharp localization to the Z ring (Fig. 5h, Table 1). At two positions (aa 333 and 348) we compared YFP and GFP insertions. The YFP was sharply localized while the GFP insert was much more diffuse (Fig. 5l, m).

Although 333ins-YFP was functional for cell division under complementing condition, it showed dominant negative effects when overexpressed with endogenous FtsZ. The dominant negative effects of 333ins-YFP were significantly

stronger than those of the N- or C-terminal-YFP fusion, or wild-type FtsZ, in both colony and cell elongation assays.

N- and C-terminal domains

To consolidate and summarize the analysis, we constructed the N-terminal domain comprising aa 1–195, and the C-terminal domain comprising aa 195–383 (see Discussion for our assignment of the division point). We tested them for dominant negative effects in the colony assay. Consistent with the complete set of deletion chimeras, the N-terminal domain was totally dominant negative (no colonies) at 0.02% arabinose, and gave smaller colonies at 0.002%. The C-terminal domain showed no dominant negative effects in

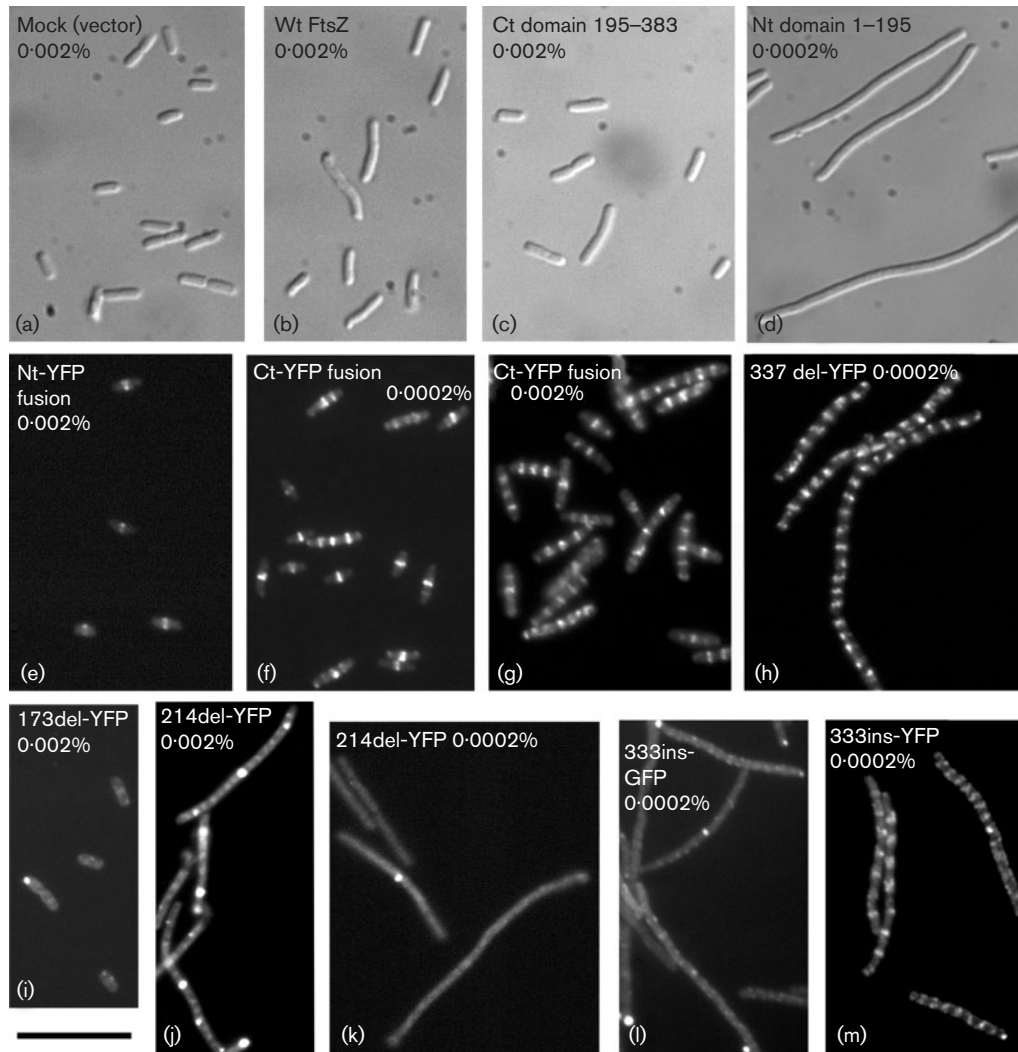


Fig. 5. Dominant negative phenotypes of various constructs grown in liquid culture with 0.002% arabinose (expressing the mutant at 3–5 times wild-type FtsZ levels) or 0.0002% arabinose (expressing the mutant at ~ 1 times wild-type levels). Cells at OD_{600} 0.5–0.7 were fixed and observed by differential-interference contrast microscopy (a–d) or by the fluorescence signal from YFP/GFP (e–m). Mock experiments with empty vector (pJSB2) (a) and cells expressing wild-type FtsZ (b) were used for controls. Overexpression of wild-type FtsZ caused very slight elongation (b). The C-terminal domain (aa 195–383) had no dominant negative effects at 0.002% arabinose (c), but the N-terminal domain (aa 1–195) produced elongated cells at 0.0002% (d). YFP-FtsZ (full-length FtsZ with N-terminal YFP) gave short cells with sharply localized Z rings at 0.002% (e). FtsZ-YFP (C-terminal YFP) gave elongated cells with multiple Z rings at 0.002% (g), but more normal-looking cells at 0.0002% (f) (however, these cells showed elongation at later times). 377delYFP, missing only the last 5 aa, produced highly elongated cells and showed very sharp localization to multiple Z rings (h). 173del-YFP, truncated in the N-terminal domain gave normal short cells and showed a diffuse distribution with occasional bright foci at 0.002% arabinose (i). 214del-YFP, truncated in the C-terminal domain produced elongated cells and showed a weak periodic pattern at 0.002% arabinose (j), but a diffuse distribution at 0.0002% arabinose with occasional bright foci (k). The GFP insertion at aa 333 in the C-terminal spacer caused cell elongation and showed a diffuse and weakly periodic localization (l). The YFP insertion at the same site showed a much brighter and sharper localization to Z rings (m). The dominant negative effects seen with this construct are probably occurring in the absence of the suppressor mutation that gave the very normal cells in complementing conditions (Fig. 3). Bar, 10 μ m.

the colony assay at any arabinose concentration. However, it may not be completely inert since it produced a barely detectable cell elongation at 0.2% arabinose, but it is definitely much weaker in effect than the N-terminal domain.

To confirm that the N- and C-terminal domains are independently folding, we expressed them in a pET system. The C-terminal domain was recovered as a soluble protein from the bacteria. The N-terminal domain was insoluble as

initially expressed, but could be solubilized in 4 M guanidine hydrochloride and renatured as a soluble protein by dialysis (G. Briscoe and H. P. Erickson, unpublished results). The initial insolubility of the N-terminal domain may be due to the high level expression from pET, since its dominant negative activity indicates that it is soluble when expressed at lower levels from pBAD.

DISCUSSION

Our original goal was to search for sites on FtsZ that could tolerate an insertion of the 27 kDa GFP protein, or a smaller 20 aa insert, using the random transposon mutagenesis technology of Sheridan *et al.* (2002). We found 16 unique insertion sites in FtsZ, and only one YFP insertion mutant in the C-terminal spacer was functional for cell division. With 333ins-YFP as the sole source of FtsZ, cells were of normal length and had normal-looking Z rings. These cells probably have a second mutation that appears with high frequency and accelerates the initial slow growth. This construct will be useful for studying FtsZ dynamics.

The failure of the other 15 inserts to function for cell division could be due to two reasons – the insert could block an essential binding reaction, or it could disrupt folding of the FtsZ protein. About half of our inserts were in the top or bottom protofilament interface, where they would sterically block FtsZ protofilament assembly. We obtained one insertion on the front and four insertions on the right side of the protofilament (Table 1). These might be blocking essential binding reactions, but we think it is more likely that their inactivity is due to misfolding of the FtsZ protein. The one insert that was functional, 333ins-YFP, is in the C-terminal spacer, which is thought to be disordered, in which case further disorder would not have an effect.

N-terminal GTP-binding domain – aa 1–195

The dominant negative effects observed provide a much stronger interpretation. The global interpretation is that the N-terminal domain, aa 1–195, is an independently folding domain that is dominant negative when expressed without a functional C-terminal domain. The C-terminal domain, aa 195–383, has no dominant negative effects when expressed by itself, even at the highest concentrations. This interpretation is consistent with our recent study of point mutants (Redick *et al.*, 2005). In that study, mutants of the bottom interface, which leave the top (N-terminus) intact, were dominant negative, while mutants of the top interface were not.

We believe that insertions or deletions within the N-terminal globular domain are not dominant negative, probably because they prevent the folding of the domain. Insertions at aa 1 and 8 deserve special attention. The first 9 aa of *E. coli* FtsZ are thought to be unstructured, based on the crystal structure of *Pseudomonas* FtsZ (Cordell *et al.*, 2003). Inserts in this segment, at aa 1 and 8, should not disrupt the folding of the rest of the protein, and indeed the

YFP insert at aa 1 (at the N-terminus) is almost not dominant negative and can co-localize to the Z ring (Ma *et al.*, 1996) (Fig. 5e). However, the insert at aa 8 is dominant negative. The X-ray structure of *Pseudomonas* FtsZ shows that *E. coli* aa 10 is close to the bottom protofilament interface. The GFP insert at aa 8 will, therefore, pose a steric block to the bottom interface, leaving a protein with only the N-terminal domain functional.

The YFP insert at aa 195 was dominant negative, implying that it could form a complete and properly folded N-terminal domain. The simple truncation at aa 195 was also dominant negative (the truncation chimera was not, and we do not understand the reason for this). This suggests that aa 195 is at or beyond the boundary between the N- and C-terminal domains. The amino acid at position 195 is in the middle of the long alpha helix H7, which runs from aa 178–203 in *E. coli* FtsZ (Cordell *et al.*, 2003). Thus our analysis places the first half of H7 within the N-terminal domain and the second half within the C-terminal domain.

Oliva *et al.* (2004) determined the domain boundary to be much earlier in the protein sequence, at the equivalent of *E. coli* aa 179, placing the helix H7 entirely in the C-terminal domain. We prefer to assign the first part of H7, aa 178–195, to the N-terminal globular domain for two reasons. First, we believe that the highly conserved aa F182 and N186 belong to the N-terminal domain. These amino acids both contact the GTP, and have been identified as protofilament contact residues in tubulin (Nogales *et al.*, 1998; Redick *et al.*, 2005). Second, the first half of helix H7 makes extensive contact with the N-terminal domain, but does not make any contact with the C-terminal domain. The second half of H7 makes extensive contact with the C-terminal domain and seems to belong there. In support of this assignment, we have found that the N-terminal domain aa 1–179 had no dominant negative effects, whereas aa 1–195 was fully dominant negative.

C-terminal globular domain – aa 195–316

Oliva *et al.* (2004) reported that the C-terminal domain folds independently, and we confirmed this for the *E. coli* protein by obtaining the complete C-terminus, aa 195–383, as a soluble protein by expression from the pET system. Our experiments showed that this C-terminal domain had almost no dominant negative activity, causing only marginal cell elongation at 5 times the level of wild-type FtsZ. This is consistent with our previous observations with a set of 8 point mutants of the top interface. These point mutants, which should have a fully functional C-terminal domain, also had almost no dominant negative activity (Redick *et al.*, 2005).

Evidence for directional assembly

The N-terminal domain contains all of the amino acids of the top protofilament interface (Oliva *et al.*, 2004), and should be able to bind to the bottom of a protofilament or a

free FtsZ subunit. This is likely the mechanism by which it inhibits cell division. However, this block appears to be weak, since it requires 3–5 times the wild-type FtsZ level to completely poison division. As explained previously (Redick *et al.*, 2005), this actually understates the weakness. The total endogenous FtsZ in the cell is 7–10 μM , however, *in vitro* experiments predict that most of the FtsZ will be assembled into protofilaments, leaving only a ~ 1 μM pool of soluble subunits (Chen & Erickson, 2005). It would thus appear that the dominant negative effects require 20–50 μM concentrations of mutant to compete with the 1 μM free wild-type FtsZ.

One caveat is that some of the mutant proteins may not be completely soluble. We attempted to assay this by lysing bacteria with lysozyme and separating the lysates into soluble and insoluble fractions. We found this assay to be poorly reproducible, and generally about 50% of the wild-type FtsZ ended up in the insoluble fraction. A larger fraction of the mutant proteins appeared insoluble, but most mutants had a level of soluble protein equal to or somewhat less than the wild-type. Overall we don't trust the insoluble fraction because the wild-type protein should be almost 100% soluble. A more conservative statement would be that 5–50 μM mutant protein is, therefore, actually competing against the 1 μM pool of soluble wild-type subunits to produce dominant negative effects.

The C-terminal domain was even weaker, having almost no dominant negative activity at the highest concentrations achieved. Since the N- and C-terminal domains could bind to the bottom and top of a protofilament respectively, this suggests that assembly is directional, occurring primarily at the bottom end of the protofilament. Our recent study of point mutants led to the same conclusion that assembly was primarily at the bottom (Redick *et al.*, 2005). There we suggested a treadmilling mechanism, where assembly at the bottom was balanced by disassembly at the top. We now realize that there is an alternative mechanism, dynamic instability, that could also produce directional assembly. Dynamic instability is well established for microtubules (Desai & Mitchison, 1997), and was recently suggested for the bacterial actin homologue ParM (Garner *et al.*, 2004). In dynamic instability the polymer grows continuously for some period, and then undergoes a catastrophe and disassembles. If FtsZ does operate by dynamic instability, our results suggest that the growth phase occurs primarily at the bottom end of the protofilament. Disassembly could occur at either end.

The C-terminal spacer and the FtsA/ZipA-binding peptide

Previous studies have shown that FtsZ constructs missing the short FtsA/ZipA-binding peptide (aa 366–383) are not functional for cell division, and further are dominant negative (Din *et al.*, 1998; Ma & Margolin, 1999; Wang *et al.*, 1997). Our work confirms these findings for the constructs truncating at aa 377.

The segment between this C-terminal peptide and the main globular domains, aa 317–366, has been thought to be flexible and unstructured (reviewed by Erickson, 2001). Vaughan *et al.* (2004) referred to this segment as a 'spacer'. The hypothesis of flexibility is based on the extreme variation in length and sequence across species, and that no secondary structure is indicated by sequence analysis, or from the X-ray crystal structures of bacterial FtsZ (Cordell *et al.*, 2003; Leung *et al.*, 2004) [the first 10 aa of the spacer appear as a loop and short alpha helix in the *Thermotoga* structure (Oliva *et al.*, 2004)].

At aa 333, both the YFP and the 20 aa insert were functional for cell division, as expected for inserts in a flexible, disordered segment. However, the YFP insert at aa 326, and both inserts at aa 348 were non-functional. The amino acid at position 326 is only 10 aa from the C-terminal globular domain, and YFP here may be posing a steric block to a binding interaction near aa 316. We did not have a 20 aa insert at this position. The amino acid at position 348 may be a site where the spacer has some structure or binding interaction. The structure of the spacer deserves additional attention.

The C-terminal segment, from aa 317–383, is not needed for protofilament assembly. Wang *et al.* (1997) reported that FtsZ 1–320 assembled into protofilaments, and we have found the same thing for FtsZ 1–316 (Y. Chen and H. P. Erickson, unpublished observations). Inserts or truncations in this segment should co-assemble with the endogenous FtsZ, and this is indicated by the sharp localization to the Z ring of all YFP inserts. It is not clear why these constructs have dominant negative effects when overexpressed with endogenous FtsZ.

The superiority of Venus-YFP and the efficiency of transposon insertion

The YFP construct that we used, Venus, has been claimed to fold better and faster than other GFP variants (Nagai *et al.*, 2002). Consistent with this we found three significant advantages of Venus-YFP over GFP. First, the Venus-YFP transposon gave a 3 times higher frequency of fluorescent colonies than GFP. Second, the Venus-YFP insertion at aa 333 was functional for cell division, while the GFP insertion at that point failed to complement. Third, in dominant negative conditions, the Venus-YFP inserts at aa 333 (Fig. 5g, h) and 348 (data not shown) showed much sharper localization to the Z ring than did the GFP inserts. Initially we compared Venus-YFP to eGFP [originally GFPmut1, F64L/S65T (Cormack *et al.*, 1996), but additionally modified by Clontech]. The GFP used for the original localization of FtsZ-GFP (Ma *et al.*, 1996), as well as the analysis of Z-ring dynamics (Anderson *et al.*, 2004; Stricker *et al.*, 2002), was GFPmut2 (S65A/V68L), which has significantly faster folding and stability than eGFP in bacterial cells (Cormack *et al.*, 1996). We therefore tested GFPmut2 at aa 333, and found that it did not complement.

We conclude that Venus-YFP is superior to eGFP and GFPmut2 for function in bacteria.

At 3 of the 16 unique sites we obtained 2 independent insertions, suggesting that the insertional mutagenesis was nearly saturated. Similarly Sheridan *et al.* (2002) obtained multiple insertions at several sites. This raises the question of why we obtained insertions at only 16 of the 383 aa. This may be due to sequence bias for transposon insertion (Reznikoff *et al.*, 1999). If so, it raises a caveat that, although the insertions target random locations in the protein, they actually sample only a small fraction of all possible locations. It may, therefore, be useful to supplement a transposon-based insertion study with a few judiciously designed insertions based on the X-ray structure.

ACKNOWLEDGEMENTS

We thank Dr Thomas E. Hughes for providing the materials and a detailed protocol for the transposon insertion. We thank Dr Atsushi Miyawaki for the vector with YFP Venus. We thank Gina Briscoe, Duke University Medical Center, for assistance in preparing the N- and C-terminal domains in the pET expression system. The work was supported by NIH grant GM-66014.

REFERENCES

- Anderson, D. E., Gueiros-Filho, F. J. & Erickson, H. P. (2004). Assembly dynamics of FtsZ rings in *Bacillus subtilis* and *Escherichia coli* and effects of FtsZ-regulating proteins. *J Bacteriol* **186**, 5775–5781.
- Chen, Y. & Erickson, H. P. (2005). Rapid *in vitro* assembly dynamics and subunit turnover of FtsZ demonstrated by fluorescence resonance energy transfer. *J Biol Chem* **280**, 22549–22554.
- Chen, Y., Bjornson, K., Redick, S. D. & Erickson, H. P. (2005). A rapid fluorescence assay for FtsZ assembly indicates cooperative assembly with a dimer nucleus. *Biophys J* **88**, 505–514.
- Cordell, S. C., Robinson, E. J. & Lowe, J. (2003). Crystal structure of the SOS cell division inhibitor SulA and in complex with FtsZ. *Proc Natl Acad Sci U S A* **100**, 7889–7894.
- Cormack, B. P., Valdivia, R. H. & Falkow, S. (1996). FACS-optimized mutants of the green fluorescent protein (GFP). *Gene* **173**, 33–38.
- Dai, K. & Lutkenhaus, J. (1991). *ftsZ* is an essential cell division gene in *Escherichia coli*. *J Bacteriol* **173**, 3500–3506.
- Datta, P., Dasgupta, A., Bhakta, S. & Basu, J. (2002). Interaction between FtsZ and FtsW of *Mycobacterium tuberculosis*. *J Biol Chem* **277**, 24983–24987.
- Desai, A. & Mitchison, T. J. (1997). Microtubule polymerization dynamics. *Annu Rev Cell Dev Biol* **13**, 83–117.
- Din, N., Quardokus, E. M., Sackett, M. J. & Brun, Y. V. (1998). Dominant C-terminal deletions of FtsZ that affect its ability to localize in *Caulobacter* and its interaction with FtsA. *Mol Microbiol* **27**, 1051–1063.
- Erickson, H. P. (1998). Atomic structures of tubulin and FtsZ. *Trends Cell Biol* **8**, 133–137.
- Erickson, H. P. (2001). The FtsZ protofilament and attachment of ZipA-structural constraints on the FtsZ power stroke. *Curr Opin Cell Biol* **13**, 55–60.
- Erickson, H. P., Taylor, D. W., Taylor, K. A. & Bramhill, D. (1996). Bacterial cell division protein FtsZ assembles into protofilament sheets and minirings, structural homologs of tubulin polymers. *Proc Natl Acad Sci U S A* **93**, 519–523.
- Garner, E. C., Campbell, C. S. & Mullins, R. D. (2004). Dynamic instability in a DNA-segregating prokaryotic actin homolog. *Science* **306**, 1021–1025.
- Harry, E. J. (2001). Bacterial cell division: regulating Z-ring formation. *Mol Microbiol* **40**, 795–803.
- Khlebnikov, A., Datsenko, K. A., Skaug, T., Wanner, B. L. & Keasling, J. D. (2001). Homogeneous expression of the P_{BAD} promoter in *Escherichia coli* by constitutive expression of the low-affinity high-capacity AraE transporter. *Microbiology* **147**, 3241–3247.
- Leung, A. K., Lucile White, E., Ross, L. J., Reynolds, R. C., DeVito, J. A. & Borhani, D. W. (2004). Structure of *Mycobacterium tuberculosis* FtsZ reveals unexpected, G protein-like conformational switches. *J Mol Biol* **342**, 953–970.
- Levin, P. A. & Losick, R. (1996). Transcription factor Spo0A switches the localization of the cell division protein FtsZ from a medial to a bipolar pattern in *Bacillus subtilis*. *Genes Dev* **10**, 478–488.
- Ma, X. & Margolin, W. (1999). Genetic and functional analyses of the conserved C-terminal core domain of *Escherichia coli* FtsZ. *J Bacteriol* **181**, 7531–7544.
- Ma, X., Ehrhardt, D. W. & Margolin, W. (1996). Colocalization of cell division proteins FtsZ and FtsA to cytoskeletal structures in living *Escherichia coli* cells by using green fluorescent protein. *Proc Natl Acad Sci U S A* **93**, 12998–13003.
- Margolin, W. (2001). Spatial regulation of cytokinesis in bacteria. *Curr Opin Microbiol* **4**, 647–652.
- Nagai, T., Iyata, K., Park, E. S., Kubota, M., Mikoshiba, K. & Miyawaki, A. (2002). A variant of yellow fluorescent protein with fast and efficient maturation for cell-biological applications. *Nat Biotechnol* **20**, 87–90.
- Nogales, E., Downing, K. H., Amos, L. A. & Lowe, J. (1998). Tubulin and FtsZ form a distinct family of GTPases. *Nat Struct Biol* **5**, 451–458.
- Oliva, M. A., Cordell, S. C. & Lowe, J. (2004). Structural insights into FtsZ protofilament formation. *Nat Struct Mol Biol* **11**, 1243–1250.
- Redick, S. D., Stricker, J., Briscoe, G. & Erickson, H. P. (2005). Mutants of FtsZ targeting the protofilament interface: effects on cell division and GTPase activity. *J Bacteriol* **187**, 2727–2736.
- Reznikoff, W. S., Bhasin, A., Davies, D. R., Goryshin, I. Y., Mahnke, L. A., Naumann, T., Rayment, I., Steinger-White, M. & Twining, S. S. (1999). Tn5: a molecular window on transposition. *Biochem Biophys Res Commun* **266**, 729–734.
- Romberg, L., Simon, M. & Erickson, H. P. (2001). Polymerization of FtsZ, a bacterial homolog of tubulin. Is assembly cooperative? *J Biol Chem* **276**, 11743–11753.
- Sheridan, D. L., Berlot, C. H., Robert, A., Inglis, F. M., Jakobsdottir, K. B., Howe, J. R. & Hughes, T. E. (2002). A new way to rapidly create functional, fluorescent fusion proteins: random insertion of GFP with an *in vitro* transposition reaction. *BMC Neurosci* **3**, 7.
- Stricker, J. & Erickson, H. P. (2003). *In vivo* characterization of *Escherichia coli ftsZ* mutants: effects on Z-ring structure and function. *J Bacteriol* **185**, 4796–4805.
- Stricker, J., Maddox, P., Salmon, E. D. & Erickson, H. P. (2002). Rapid assembly dynamics of the *Escherichia coli* FtsZ-ring demonstrated by fluorescence recovery after photobleaching. *Proc Natl Acad Sci U S A* **99**, 3171–3175.
- Vaughan, S., Wickstead, B., Gull, K. & Addinall, S. G. (2004). Molecular evolution of FtsZ protein sequences encoded within the genomes of archaea, bacteria, and eukaryota. *J Mol Evol* **58**, 19–29.
- Wang, X. D., Huang, J. A., Mukherjee, A., Cao, C. & Lutkenhaus, J. (1997). Analysis of the interaction of FtsZ with itself, GTP, and FtsA. *J Bacteriol* **179**, 5551–5559.